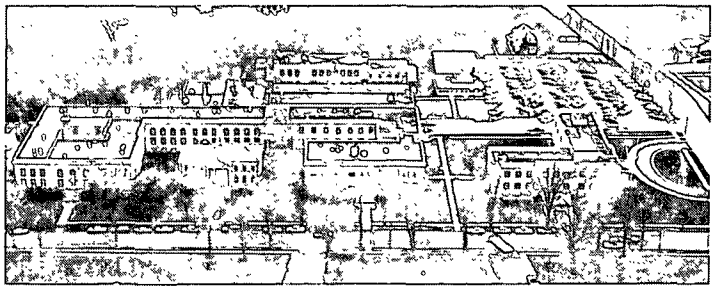

THE INSTITUTE OF PAPER CHEMISTRY, APPLETON, WISCONSIN

IPC TECHNICAL PAPER SERIES

NUMBER 317

REACTION OF Na_2CO_3 FUME PARTICLES WITH SO_2 AND O_2

GREG P. MAULE AND JOHN H. CAMERON

JANUARY, 1989

Reaction of Na_2CO_3 Fume Particles with SO_2 and O_2

Greg P. Maule and John H. Cameron

Portions of this work were used by GPM as partial fulfillment of the requirements for the Master of Science degree at The Institute of Paper Chemistry. This manuscript has been submitted for consideration for publication in the Journal of Pulp and Paper Science

REACTION OF Na_2CO_3 FUME PARTICLES WITH SO_2 AND O_2

Greg P. Maule and John H. Cameron
The Institute of Paper Chemistry
Appleton, Wisconsin 54912

ABSTRACT

This paper describes the reaction of Na_2CO_3 fume particles with SO_2 and O_2. This was the first time the reaction has been studied using fume particles similar to those in the kraft recovery boiler. The sodium carbonate fume was generated by purging a N_2/air mixture through a Na_2CO_3-Na_2S melt. Kinetic data were obtained by following the weight gain of the sample as the reaction progressed. The activation energy for the reaction was 5522 cal/mole. The rate limiting mechanism was diffusion through the product layer. The reaction was first order with respect to SO_2 and zeroth order with respect to O_2. Sulfation of the carbonate particles caused considerable sintering of the particles at relatively low temperatures. The degree of sintering increased as the fraction conversion increased. The data were accurately described by the unreacted shrinking core model for both kinetic and diffusion control.

INTRODUCTION

In the kraft recovery furnace elemental sodium is vaporized during the combustion of black liquor and becomes the base chemical for the formation of the fume in the furnace flue gases. There are two primary sources for the sodium based fumes: the inflight burning of the black liquor particles and the combustion reactions in the char bed. The fume particles are predominantly Na_2CO_3 and Na_2SO_4 with particle diameters in the range 0.25 to 1.00 μm (1). The reaction of Na_2CO_3 fume particles to form Na_2SO_4 is responsible for the capture and control of sulfur dioxide. Sulfur is released from the black liquor primarily as hydrogen sulfide. The hydrogen sulfide is oxidized in the flue gases to SO_2, which then reacts with Na_2CO_3 fume to form Na_2SO_4. Fume comprises approximately 96% of the total precipitator dust, and more than 90% of this fume is in the form of Na_2SO_4 (2). The capture of SO_2 also reduces the formation of sticky deposits in the upper boiler or in the precipitator by reducing the SO_2 partial pressure (3).

The formation of fume also has negative effects on the operation of the recovery boiler. The fume can form deposits on the heat transfer surfaces, which reduces the heat transfer rates and can possibly lead to plugging of the gas passages. About 3 to 8% of the total steam production is used to remove these deposits from the heat transfer surfaces (4).

This report describes the results of a kinetic study between Na_2CO_3 fume particles and SO_2 in the presence of O_2. The effects of temperature and gas concentration on the reaction rate were determined along with the products of the reaction and the rate limiting mechanism.

LITERATURE REVIEW

The reaction between sodium carbonate and gaseous sulfur dioxide has been studied extensively by researchers in the power-generating industry. Their concern was the elimination of SO_2 from the flue gases by adsorption on solid Na_2CO_3 or in a Na_2CO_3 melt. Although the experimental conditions are not applicable to the kraft furnace, the data obtained through these studies aid in understanding the interactions between Na_2CO_3 and SO_2 and the formation of Na_2SO_4.

This research indicates that Na_2CO_3 reacts with SO_2 to form Na_2SO_3 without O_2 present and reacts with SO_2 to form Na_2SO_4 when O_2 is present. Butler and Waites (5) studied the reaction by passing SO_2 over solid Na_2CO_3 in the absence of oxygen. Above 300°C they found that the SO_2 reacted rapidly with the Na_2CO_3 to form Na_2SO_3.

Smith and Kumura (6) conducted a study similar to Butler and Waites (5). The reaction was studied in the temperature range of 80 to 140°C. Throughout this temperature range approximately all the Na_2CO_3 was converted to Na_2SO_3 in a time period of 60 seconds. A key variable in this study was the dependence of the Na_2CO_3 reactivity on the origin of the Na_2CO_3. They prepared the Na_2CO_3 by thermal decomposition of $NaHCO_3$. When decomposed at 473°C the Na_2CO_3 had a different crystal structure and it was substantially more reactive than Na_2CO_3 prepared at 453°C.

Davis and Keener (7) studied the overall reaction between Na_2CO_3 and SO_2 in the presence of O_2. They experimented with particles that had diameters of 20, 90, and 200 μm. The temperature ranged from 121 to 344°C. The reaction rate depended heavily on the particle size. This increase in reactivity for the smaller particles was assumed to be directly related to the increase in surface area per unit mass for the smaller particles. For the 90 μm size particle the activation energy was calculated to be 23,948 cal/mol. The reaction was first order with respect to the SO_2 concentration, and the rate limiting mechanism was diffusion through the solid product layer. Above 344°C the effects of sintering had begun to inhibit the reaction.

Backman et al. (8) used a thermogravimetric method to continuously follow the reaction of Na_2CO_3 particles with SO_2 and O_2. Sintering of the Na_2CO_3 particles above 450°C caused significant reduction of the active surface area and thus resulted in a decrease in the reaction rate. To avoid this problem all samples were presintered at 650°C for 12 hours. The temperature range studied was 350 to 700°C. The average diameter of the Na_2CO_3 particles was 55 μm with a specific surface of 0.132 m^2/g. The activation energy was determined to be 15,535 cal/mol. The reaction rate was first order with respect to the SO_2 concentration and zeroth order with respect to O_2 concentration. Sodium sulfate was the kinetically favored compound formed. The overall reaction rate also depended on the manner of preparation of Na_2CO_3.

These studies indicate that Na_2SO_4 is the product of the reaction between SO_2, O_2, and Na_2CO_3 and that this reaction is first order in SO_2. However, these studies also show that this reaction is highly dependent on the size and origin of the Na_2CO_3 particles. This is further illustrated by the study of Mocek et al. (9) that the reaction rate of SO_2 with Na_2CO_3 may vary by several

orders of magnitude depending on the source of the Na_2CO_3. The more reactive form of Na_2CO_3 was made by thermal decomposition of $NaHCO_3$.

Since this reaction is highly dependent on the source and particle size of the Na_2CO_3, these studies are not applicable to the sulfation as it occurs within the kraft furnace. Recently, Cameron (1) has found that Na_2CO_3 fume particles similar in size and appearance to those found within the kraft furnace are generated during the oxidation of Na_2S in a Na_2CO_3 melt. This ability to generate these Na_2CO_3 fume particles provides the opportunity of studying the reaction between Na_2CO_3 and SO_2 with particles similar to those found within the kraft furnace.

The purpose of this study was to determine how the fractional conversion of Na_2CO_3 fume particles changed with time at variable reactant gas concentration and temperature, and to identify the rate-limiting physical or chemical step. The overall reaction of Na_2CO_3 being considered is shown below.

$$Na_2CO_{3(s)} + SO_{2(g)} \xrightarrow{O_2} Na_2SO_{4(s)} + CO_{2(g)} \qquad (1)$$

The unreacted shrinking core model was used in this study to determine the relationship between the time of reaction and the extent of conversion of the Na_2CO_3 with variable SO_2 concentration and temperature.

EXPERIMENTAL APPARATUS

The experiment consisted of two distinct process steps. First, the Na_2CO_3 fume was generated and collected on a glass fiber filter paper. Second, the filter paper containing the Na_2CO_3 fume particles was placed in a fixed bed reactor to react with SO_2 and O_2. The reaction was followed by measuring the amount of weight gained at variable times.

FUME GENERATION

The experimental system used to generate the fume was developed by Cameron et al. (1). The system is shown in Figure 1. The reactor was a cylindrical ceramic crucible 5.0 cm in diameter and approximately 10 cm in length. The reactor was charged with approximately 80 grams of Na_2CO_3 and 3.0 grams of Na_2S. An induction furnace was used to heat and maintain the reactor at approximately 927°C. During the heating phase, the salts were purged with N_2. At 927°C the melt was oxidized using an air/nitrogen purge. Once fuming started there was a three to five minute delay before the fume samples were collected. The samples were collected on a preweighed 2.54-cm diameter glass fiber filter paper and stored in a desiccator under a nitrogen atmosphere. The fume appeared similar in size to that found within the recovery boiler, with the particle diameter between 0.25 and 1.0 μm. Analysis of this fume indicated that it was essentially pure Na_2CO_3.

Figure 1 here

REACTOR

A fixed-bed reactor was used to study the reaction of Na_2CO_3 with SO_2 and O_2. The purpose of the experiment was to determine the rate limiting mechanism and the effects of temperature and gas concentration (SO_2, O_2) on the overall reaction with Na_2CO_3 fume particles to form Na_2SO_4 fume:

$$Na_2CO_{3(s)} \xrightarrow{SO_2,\ O_2} Na_2SO_{4(s)} \qquad (2)$$

The fixed-bed reactor system is shown in Figure 2. The equipment used for the reactor consisted of a Type 316 stainless steel tube 5.08 cm in diameter and 76 cm in length. The reactant gas used entered through the bottom of the

tube. The initial 30 cm of the stainless steel tube contained ceramic packing to ensure good mixing and uniform heating of the gases. A thermocouple was inserted into the gas inlet stream and through the ceramic packing to monitor the temperature of the gas in the cylinder. A housing was mounted on the top of the tube to allow for easy access to the fume samples and good contact between the reactant gases and the sample. The filter paper, with the fume sample on it, was placed in the housing and sealed with brass and Teflon gaskets to ensure that all the reactant gas flowed through the sample and not around it. The reaction temperature was measured using a Chromel-Alumel thermocouple which was inserted through the upper housing and placed in contact at the backside of the filter paper.

Figure 2 here

The reactant gas consisted of research grade N_2, air, and SO_2. Calibrated rotometers were used to adjust the reactant gas mixture to the desired composition. The system was heated using an electric furnace.

Each reaction experiment included four steps: 1. a heating phase during which the sample was heated to the desired reaction temperature while being purged with nitrogen, 2. a holding period where the sample was allowed to stabilize for ten minutes at the reaction temperature and was then weighed to determine the weight loss due to additional drying and some particle loss, 3. the isothermal reaction phase during which the nitrogen purge was shut off and the properly adjusted reactant gas mixture was turned on and allowed to react for a prescribed amount of time, and 4. a purging phase during which the gas flow was shut off and the sample was purged with N_2 for three minutes, and then weighed to determine the weight gain.

ANALYSIS

Ion chromatography and x-ray diffraction analysis were used to determine the composition of the reacted samples. The chemical analysis from both techniques indicated that Na_2SO_4 was the predominant species formed in the reaction. In calculating the percent conversion, from the measured weight gain, the entire sample weight gain would be assumed to result from Na_2SO_4 formation. Specific surface area analysis was done using a dynamic N_2 absorption method. The measurements were made on the Na_2CO_3 fume particles only. The analysis was conducted with the fume on the filter paper; therefore, the area in contact with the filter paper may not have been accounted for in the test. The fume samples on the filter papers had specific surface areas of 6.56 m^2/g.

INITIAL EXPERIMENTATION

A study was conducted to determine the operating conditions at which external mass transfer through the gas boundary and interparticle mass transfer resulting from particle-particle contact would be negligible. The only resistances included in the unreacted shrinking core model were mass transfer through the porous product layer and the chemical reaction rate.

EXPERIMENTAL MEASUREMENTS

The results of the study include conversion versus time data for variable temperatures, sulfur dioxide concentration, and oxygen concentration. The temperatures studied were 121, 149, 177, 205, 224, and 246°C. At each temperature, conversion versus time data were collected at sulfur dioxide concentrations of 0.43, 0.349, and 0.249% and an oxygen concentration of 1.00%. Also, at each temperature, conversion versus time data were collected at oxygen concentrations of 2.15, 1.00, and 0.34%, and a sulfur dioxide concentration of 0.43%.

RESULTS OF THE MEASUREMENTS

EFFECT OF PARTICLE LOADING AND GAS FLOW RATE

The effect of particle loading was studied by measuring the reaction rate at different particle loadings. At particle loadings above 0.0150 g, the rate of Na_2CO_3 conversion to Na_2SO_4 significantly decreased with an increase in particle loading. The effect of gas flow rate on the conversion of Na_2CO_3 was studied by measuring the conversion rate at gas flow rates ranging from 240 to 465 cc/min. The conversion rate was unaffected by gas flow rates above 330 cc/min. Below this gas flow rate there was a decrease in reaction rate with a decrease in gas flow rate. To ensure that interparticle diffusion did not significantly affect the reaction, the experimental data were obtained at particle loadings of 0.0150 g and gas flow rates of 330 cc/min.

EFFECT OF TEMPERATURE

The time versus conversion data for the Na_2CO_3 fume particle at six different temperatures are shown in Figure 3. The reactant gas composition was 0.43% SO_2, 1.0% O_2, and 98.57% N_2. The reaction increased with temperature throughout the temperature range studied. The weight gained as a result of reaction is shown as fraction conversion of Na_2CO_3 to Na_2SO_4 according to Reaction (1). At large reaction times, conversion increased and the slope gradually decreased. This occurred as a result of two processes. First, as the reaction progressed, diffusion resistance through the porous product layer increased. Second, as revealed by scanning-electron microscopy, a significant degree of sintering occurred as a result of the conversion of Na_2CO_3 to Na_2SO_4.

Figure 3 here

The unreacted shrinking core model, under chemically controlled conditions, was used to determine the rate constant for the reaction at each temperature. An Arrhenius plot of the natural logrithm of the rate constant versus reciprocal temperature is shown in Figure 4. The graph is linear with an activation energy of 5522.5 cal/g mol.

Figure 4 here

The experimental data were fit to the unreacted shrinking core model, which included the effects of both the intrinsic reaction rate and diffusion through the porous product layer. The effective diffusivity was found to equal 5.589 x 10^{-7} cm^2/min. The final relationship between time, temperature, and the extent of reaction is given by:

$$t = (5.96 \times 10^{-7})/(kC_{Ab})\ [1-(1-X_B)^{1/3}]\ [1 + 7.4545k\{(1-X_B)^{1/3} + 1-2(1-X_B)^{2/3}\}] \quad (3)$$

The fit of Eq. (3) to the experimental data is shown in Figure 5. The expression described the reaction of Na_2CO_3 with SO_2 and O_2 quite well.

Figure 5 here

THE EFFECT OF SO_2 CONCENTRATION

The influence of the concentration of SO_2 was also studied at a constant reaction temperature of 177°C. The reaction was conducted with 0.249, 0.349, and 0.43% SO_2 in the gaseous reactant stream with 1.00% O_2. Figure 6 shows the congruency of the experimental model to the reaction data at each SO_2 concentration.

Figure 6 here

The congruency of Eq. (3) to the experimental data suggests that the assumption of a first order overall reaction was valid. To further prove this, the effects of variable SO_2 concentration and variable O_2 concentration were studied using a homogeneous model to determine the overall reaction order. The order of reaction was determined from the slope of the plot of ln (r) versus ln (SO_2). The reaction rate, "r" was determined by the initial slope of the time versus fraction conversion curve. The slope was obtained by a linear regression analysis. The plot of the ln (r) versus ln (SO_2) is shown in Figure 7. The slope of the curve is 0.989, which indicated a first order reaction with respect to SO_2 at the conditions studied.

Figure 7 here

EFFECT OF O_2

The effect of O_2 on the reaction rate of Na_2CO_3 fume particles was studied at 177°C. To determine the reaction order with respect to the O_2 content of the reactant gas, the O_2 concentration was varied from 0.344 to 2.15%. The SO_2 concentration was kept constant at 0.43%. The reaction order with respect to O_2 was determined by plotting ln (rate) versus ln (O_2). The plot is shown in Figure 8. The reaction order was approximately 0.015, so it was assumed that the reaction order was zeroth order with respect to O_2.

Figure 8 here

A zeroth reaction order indicated that oxygen was involved in a fast reaction step which did not act to control the overall rate. Also, the fact that no Na_2SO_3 was found in the reacted samples indicated that the reaction rate was dependent on the relative reactivity of Na_2CO_3 toward SO_2 and was not dependent on oxygen.

SURFACE STRUCTURE

To examine structural changes occurring during the reaction, scanning-electron microscopy pictures were taken at conversions from 5 to 75%. To distinguish between structural changes resulting from increased particle temperature and those resulting from the reaction of the carbonate particles with SO_2, scanning-electron microscopy pictures were also taken of the unreacted Na_2CO_3 fume and of the Na_2CO_3 fume heated at 246°C for 15 minutes.

Figure 9 is an SEM picture of the original Na_2CO_3 fume particle. SEM pictures of the reacted particles revealed significant particle growth, formation of bonds between the individual particles, and a general coarsening of the pore structure as shown in Fig. 10. At 75% conversion almost every particle was fused together forming what appeared to be a long intertwining chain of solid product with individual particles only vaguely distinguishable in the mass.

Figures 9 and 10 here

To separate the effects of heat and chemical reaction on the surface structure, a sample of unreacted Na_2CO_3 fume was heated for ten minutes at 240°F. The scanning-electron microscopy picture indicated only a very small degree of sintering at this condition, as shown in Figure 11. By comparing these figures, it is apparent that the reaction of SO_2 with Na_2CO_3 fume particles significantly affects the structure of these particles. Reacted particles were found to be highly sintered as a result of the reaction. There was a coarsening of the pores and the formation of large bonds between the individual particles.

Figure 11 here

DISCUSSION

Initially the reaction was kinetically controlled - an incremental increase in reaction time produced a proportional increase in the fraction conversion. As the reaction continued the effects of diffusion through the porous product layer and sintering influenced the reaction rate.

EFFECT OF TEMPERATURE

The effect of temperature closely followed an Arrhenius relationship. The activation energy was determined to be 5522 cal/mole. The activation energy was low compared to values noted in the literature for the reaction between Na_2CO_3 with SO_2 and O_2. One possible reason for this was the relationship that Keener and Davis found between the reaction rate and specific surface area. They observed a lower activation energy for particles with increased specific surface area. As the particle size decreased a significant increase in specific surface area resulted. For the fume samples, the particle size was roughly two orders of magnitude smaller than that used by Keener and Davis, and the specific surface area was approximately four times greater.

The low activation energy may also indicate that an adsorption-desorption process was occurring. The gas molecules can adhere to the particle surface by either physical adsorption, Van der Waals forces, or by chemical adsorption. Typical activation energies for physical adsorption would be around 6000 cal/mole (10). The physically adsorbed molecules often move into a chemically adsorbed state. The activation energy for the reaction between Na_2CO_3 fume with SO_2 and O_2 was 5522 cal/mole, which was low enough for the adsorption process to occur. Additional experimentation would be required to determine the actual

reason for the low activation energy. This subject was not investigated further in this study.

EFFECT OF SO_2 PARTIAL PRESSURE

The rate of the reaction was dependent on the SO_2 partial pressure throughout both the kinetic controlled region and the diffusion controlled region. The dependence of the initial rate on the SO_2 partial pressure indicated that SO_2 was involved in the rate determining step of the overall reaction. The diffusion controlled region was influenced by the SO_2 partial pressure as was expected. As the partial pressure increased the driving force for diffusion into the product layer increased. This directly affects the overall rate of the reaction.

EFFECT OF O_2 PARTIAL PRESSURE

The O_2 partial pressure was not involved in the rate limiting step since it had no influence on the initial rate of the overall reaction. The reason for this was that the reaction was zeroth order with respect to O_2. This was verified by fitting the data to a homogeneous model.

EFFECTS ON SURFACE STRUCTURE

Sintering was observed in the reacted samples. This could have reduced the overall reaction rate by reducing the specific surface area of the reactant substrate. The specific surface area was reduced as the individual particles were fused together to form a larger mass. The reduction in the reaction rate at higher conversions could be the result of both diffusion limitations and sintering.

Particle sintering at relatively low temperatures was found to occur as a result of the reaction between carbonate fume particles and SO_2. This indicates that high temperatures are not necessary for sintering or hardening of deposits within the kraft furnace. If Na_2CO_3 was deposited on a heat transfer surface in the kraft furnace and then reacted with SO_2 to form Na_2SO_4, a very hard, highly sintered deposit could result at relatively low temperatures.

A summary of the results found in this study are listed in Table 1.

Table 1 here

CONCLUSIONS

The following conclusions were made for the reaction of Na_2CO_3 fume particles with SO_2 and O_2 in the temperature range 120-246°F.

1. The activation energy for the reaction was 5522 cal/mole.
2. The reaction was first order with respect to SO_2.
3. The reaction was zeroth order with respect to O_2.
4. The effective diffusivity was 5.589×10^{-7} cm^2/min.
5. The unreacted shrinking core model accurately described the reaction of Na_2CO_3 fume particles with SO_2 and O_2.
6. Significant sintering of the solid particles occurred during the course of the reaction.

ACKNOWLEDGMENT

Portions of this work were used by GPM as partial fulfillment of the requirements for the Master of Science degree at The Institute of Paper Chemistry.

REFERENCES

1. Cameron, J., International Chemical Recovery Conference, New Orleans, LA, 1985.

2. Rizhinshvili, G. and Kaplun, L., Bumazh. Prom. 1:26-28(Jan., 1983).

3. Backman, R. and Hippa, M. Corrosion relation to acidic sulfates in kraft and sodium sulfite boilers. Tappi J. 67(12):60-4(1984).

4. Cameron, J. Fume generation in kraft recovery boilers. PIMA 68(3): 32-4(1986).

5. Butler, F. and Waites, I. A thermoanalytical study of the reaction between gaseous sulfur dioxide and solid sodium carbonate. 2nd European Symposium on Thermal Analysis, 1981.

6. Smith, J. and Kimura, S. Kinetics of the sodium carbonate-sulfur dioxide reaction. AIChE J. 33(9):1522(1987).

7. Davis, W. and Keener, T., J. Air Poll. Control Assocn. 34:651-4(1984).

8. Backman, R., Hupa, M., Usikartano, T., and Akedemi, A., International Chemical Recovery Conference, New Orleans, LA, 1985.

9. Mocek, K., Bares, J., Marecek, J., and Erdos, E., Coll. Czech. Chem. Comm. 38:1628(1969).

10. Atkins, P. W. Physical Chemistry. Oxford University Press, 2nd ed. Great Britain, 1982.

NOMENCLATURE

Variable

CA = The concentration of the reactant gas.

D_e = The effective diffusivity in the product layer.

E_a = The activation energy for the reaction.

k = The reaction rate constant.

k_o = The frequency factor in the Arrhenius relationship.

k_m = The external mass transfer coefficient.

M_B = The molecular weight of the solid reactant.

N_A = Moles of reactant gas A.

N_B = Moles of solid reactant B.

R = Gas constant.

r_s = Radius of the overall solid particle.

r_c = Radius of the unreacted solid core.

T = Temperature.

t = Time.

W_I = The initial weight of the fume sample plus the filter before reaction.

W_F = The final weight of the fume sample plus the filter paper at the completion of the reaction.

W_{FP} = The weight of the filter paper alone.

X_B = The fraction conversion of the solid reactant B.

τ_B = The density of the solid reactant.

Figure Captions

Figure 1. Fume generating system.

Figure 2. Fixed bed reactor.

Figure 3. Conversion vs. time, variable temperature.

Figure 4. Arrhenius plot of reaction data.

Figure 5. Conversion vs. time, shrinking core model chemical and diffusion control.

Figure 6. Shrinking core model fit to variable sulfur dioxide concentrations.

Figure 7. ln(rate) vs. $\ln(SO_2)$.

Figure 8. ln(rate) vs. $\ln(O_2)$.

Figure 9. SEM, sodium carbonate fume sample, unreacted.

Figure 10. SEM, reacted sample, 70% conversion.

Figure 11. SEM, sodium carbonate fume heated at 475°F.

Table 1. Summary of the results for the reaction of Na_2CO_3 fume with SO_2 and O_2. The average particle diameter was assumed to be 0.5 μm. Results were obtained by applying the unreacted shrinking core model to the data.

Specific surface area	6.56	m^2/g
Activation energy	5522.22	cal/mole
Frequency factor	5.47	cm/min
Effective diffusivity	5.589×10^{-7}	cm^2/min
Reaction order with respect to SO_2	0.987	
Reaction order with respect to O_2	0.015	

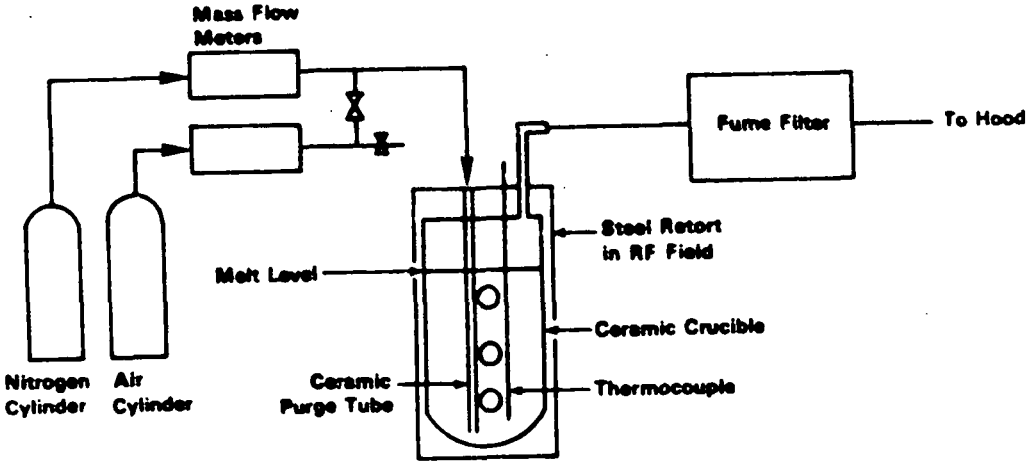

Figure 1. Fume generating system.

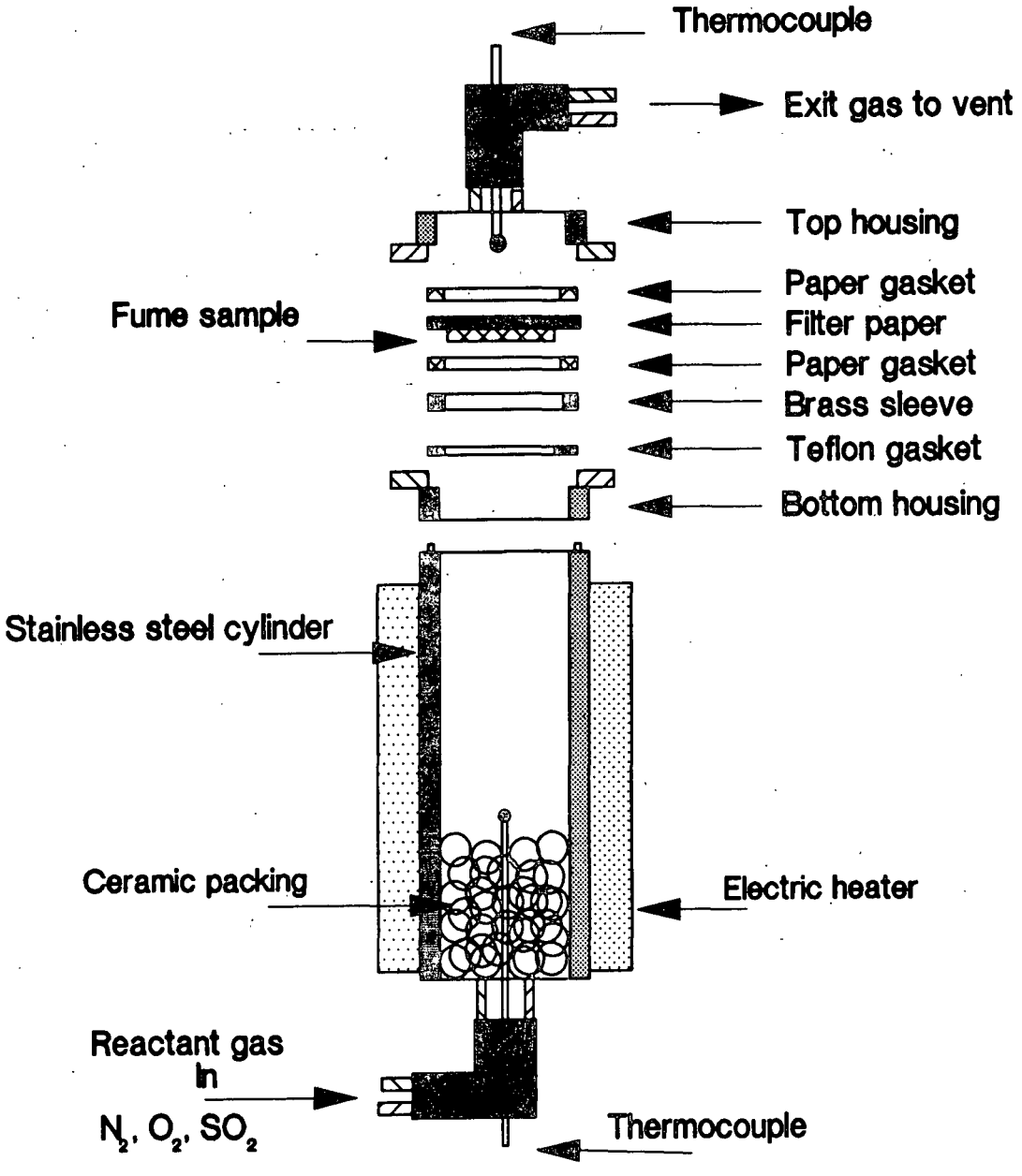

Figure 2. Fixed bed reactor.

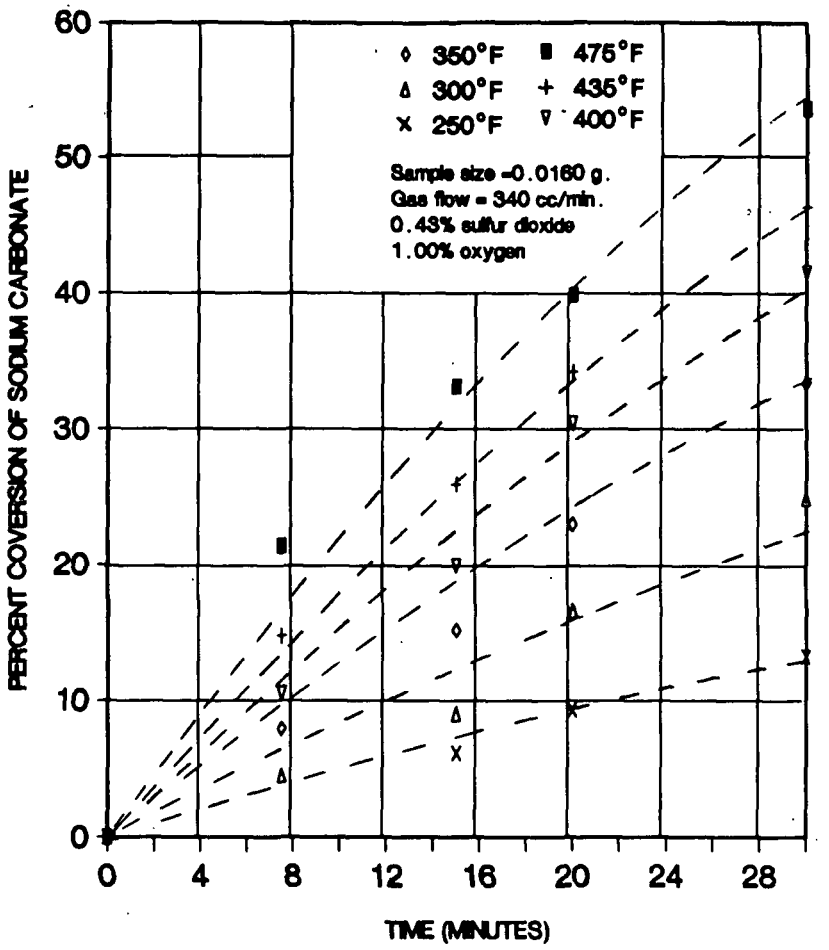

Figure 3. Conversion vs. time, variable temperature.

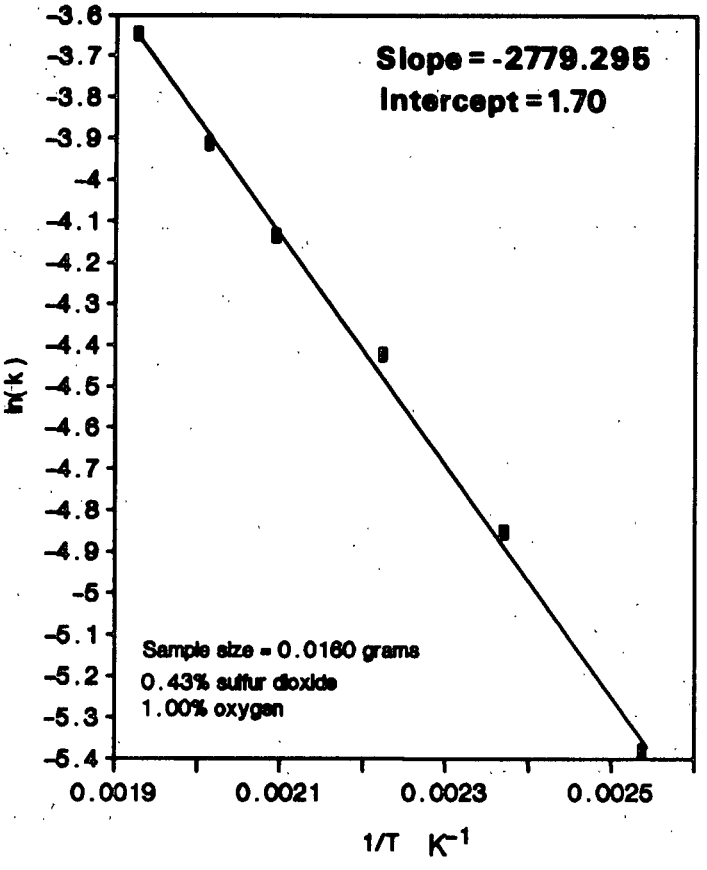

Figure 4. Arrhenius plot of reaction data.

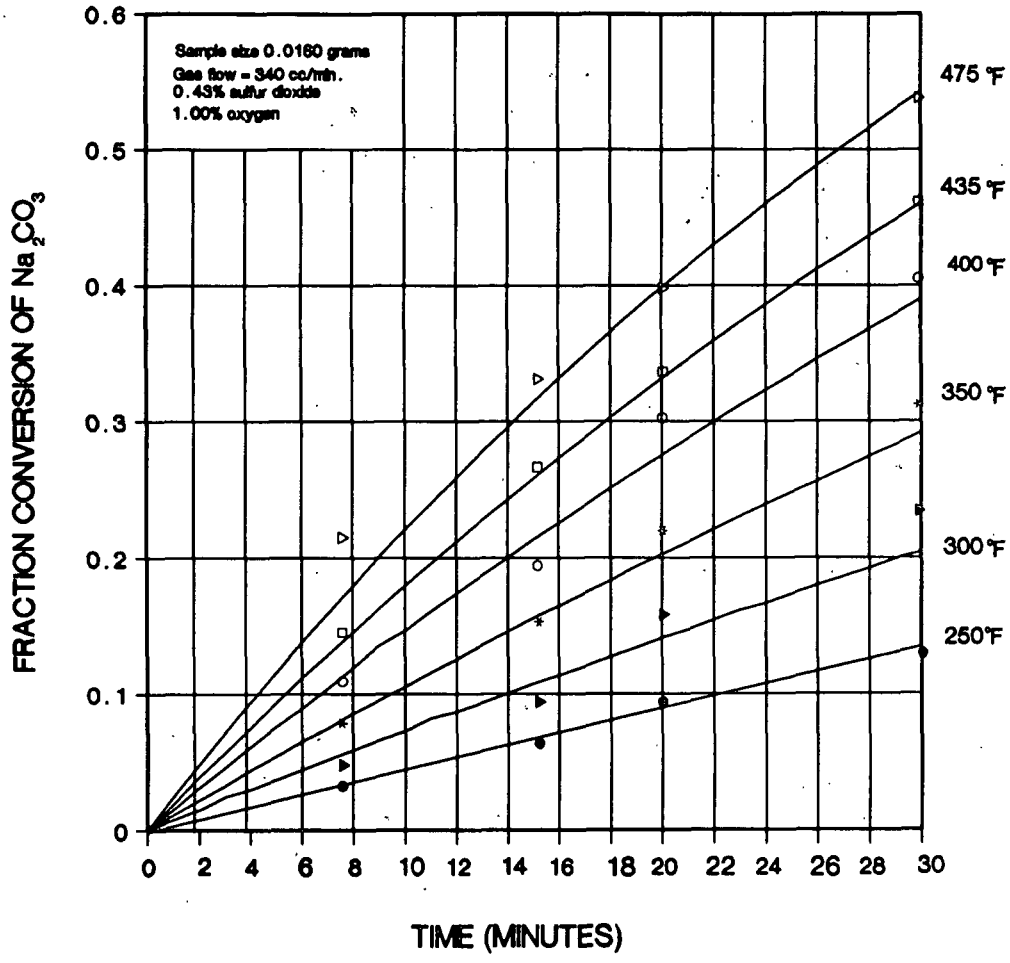

Figure 5. Conversion vs. time, shrinking core model chemical and diffusion control.

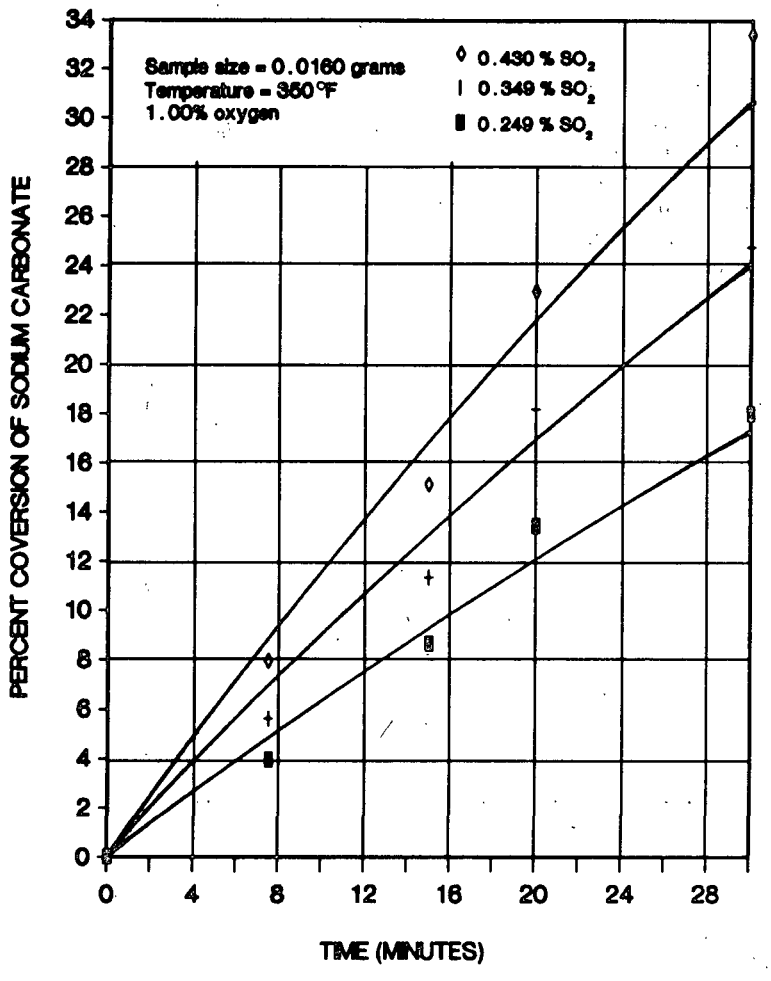

Figure 6. Shrinking core model fit to variable sulfur dioxide concentrations.

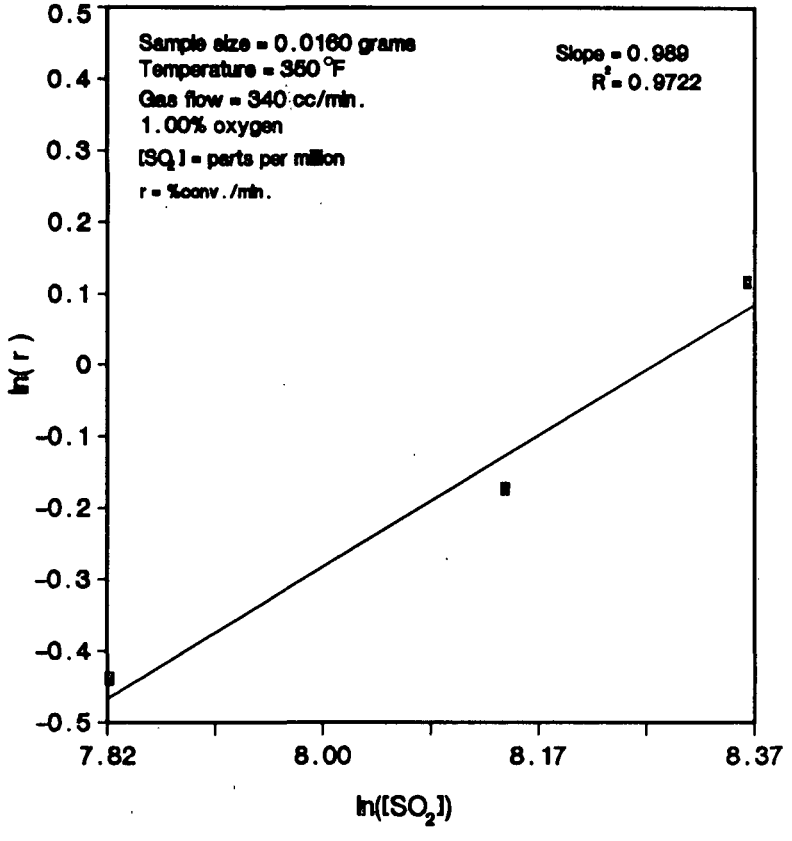

Figure 7. ln(rate) vs. $\ln(SO_2)$.

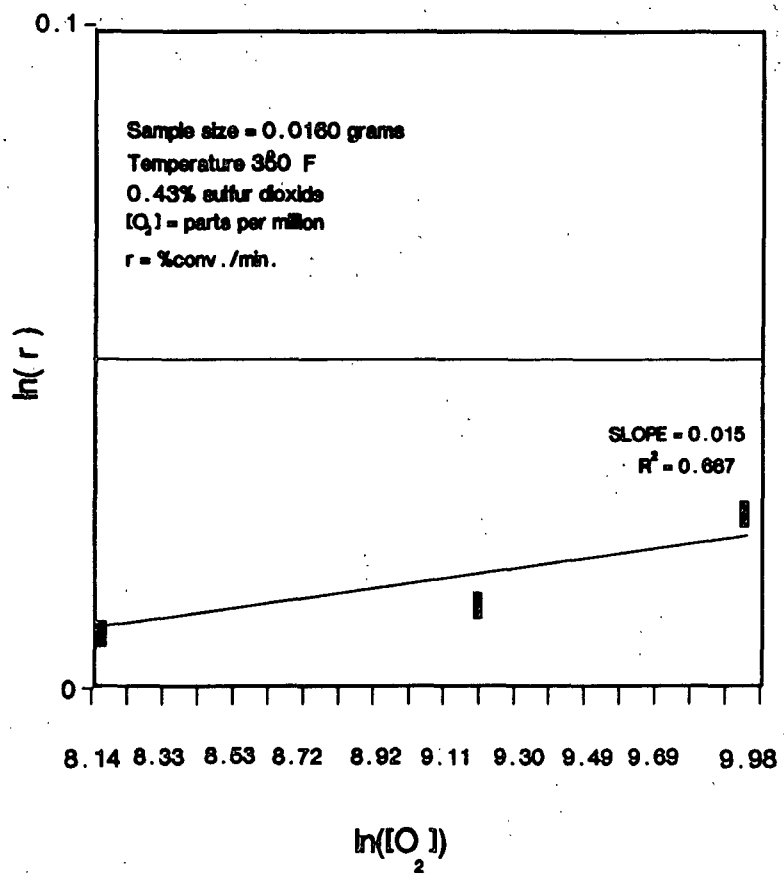

Figure 8. ln(rate) vs. $\ln(O_2)$.

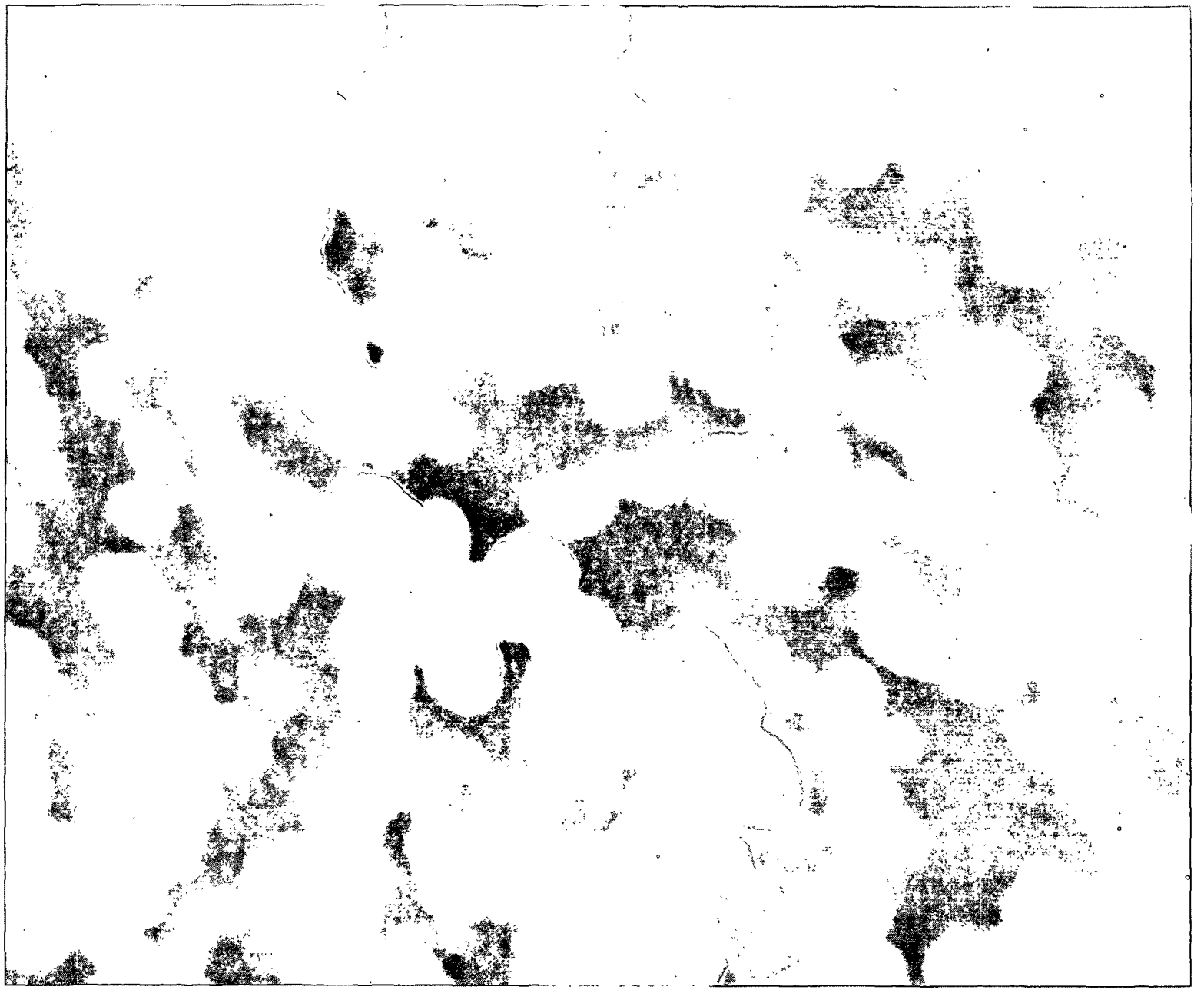

Figure 9. SEM, sodium carbonate fume sample, unreacted.

Figure 10. SEM, reacted sample, 70% conversion.

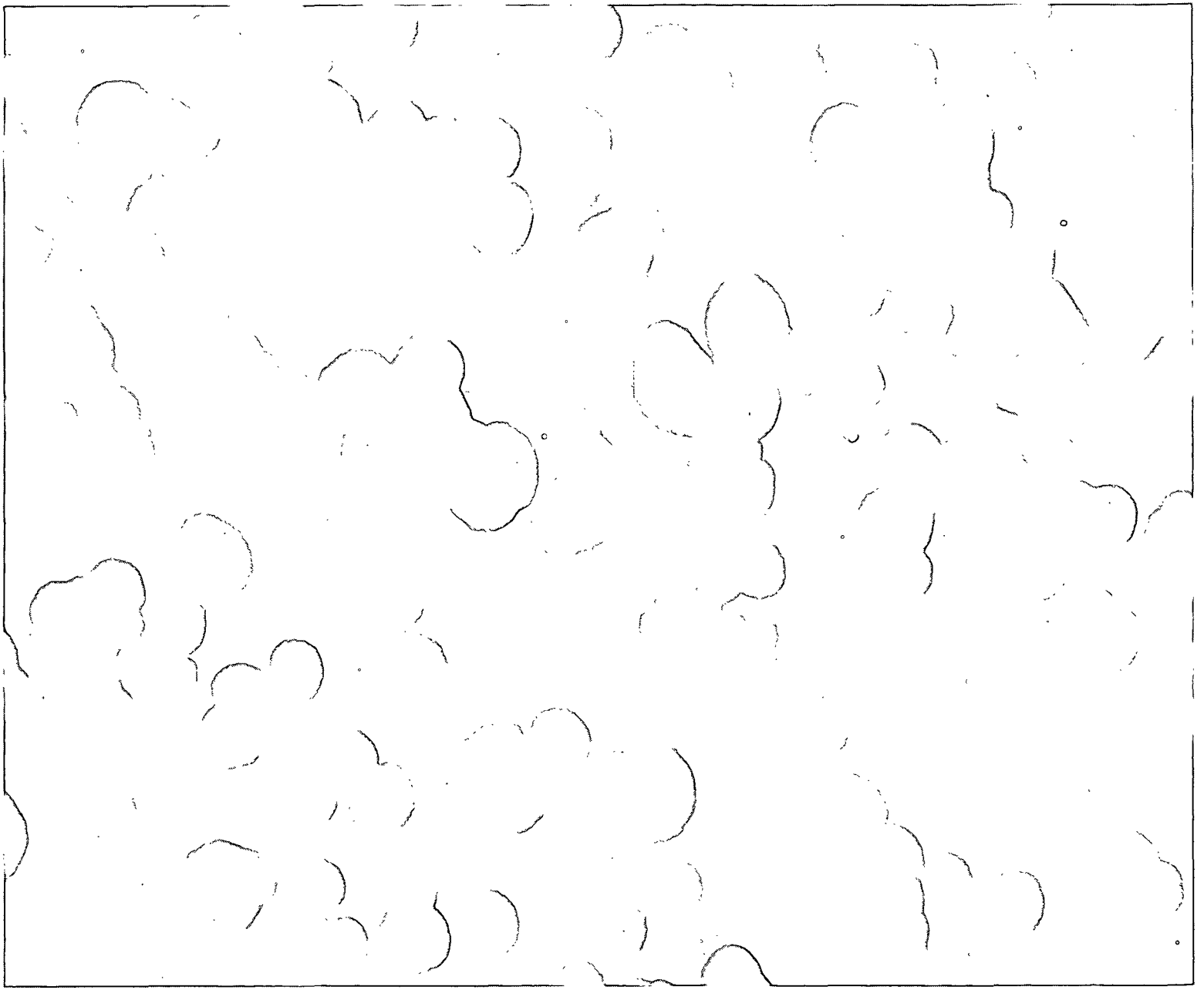

Figure 11. SEM, sodium carbonate fume heated at 475°F.